Taylor & Francis
Taylor & Francis Group

Journal of Macromolecular Science, Part A
Pure and Applied Chemistry

ISSN: 1060-1325 (Print) 1520-5738 (Online) Journal homepage: https://www.tandfonline.com/loi/lmsa20

# Optical and Vapor Sensing Properties of Calix[4]arene Langmuir-Blodgett Thin Films with Host–Guest Principles

Yaser Acikbas, Selahattin Bozkurt, Matem Erdogan, Erkan Halay, Abdulkadir Sirit & Rifat Capan

**To cite this article:** Yaser Acikbas, Selahattin Bozkurt, Matem Erdogan, Erkan Halay, Abdulkadir Sirit & Rifat Capan (2018) Optical and Vapor Sensing Properties of Calix[4]arene Langmuir-Blodgett Thin Films with Host–Guest Principles, Journal of Macromolecular Science, Part A, 55:7, 526-532, DOI: 10.1080/10601325.2018.1476824

**To link to this article:** https://doi.org/10.1080/10601325.2018.1476824

JOURNAL OF MACROMOLECULAR SCIENCE, PART A: PURE AND APPLIED CHEMISTRY
2018, VOL. 55, NO. 7, 526–532
https://doi.org/10.1080/10601325.2018.1476824



# Optical and Vapor Sensing Properties of Calix[4]arene Langmuir-Blodgett Thin Films with Host–Guest Principles

Yaser Acikbas[a], Selahattin Bozkurt[b,c], Matem Erdogan[d], Erkan Halay[b,e], Abdulkadir Sirit[f], and Rifat Capan[d]

[a]Department of Materials Science and Nanotechnology Engineering, Faculty of Engineering, University of Usak, Usak, Turkey; [b]Department of Chemistry, Scientific Analysis Technological Application and Research Center, Usak University, Usak, Turkey; [c]Department of Medical Laboratory Techniques, Vocational School of Health Services, Usak University, Usak, Turkey; [d]Department of Physics, Faculty of Science, University of Balıkesir, Balikesir, Turkey; [e]Department of Chemistry and Chemical Processing Technologies, Banaz Vocational School, Usak University, Usak, Turkey; [f]Department of Chemistry, Necmettin Erbakan University, Meram, Konya, Turkey

**ABSTRACT**

25,27-(Dipropylmorpholinoacetamido)-26,28-dihydroxycalix[4]arene was used as a chemical sensor material in this work. The calix[4]arene LB thin films were prepared onto a gold-coated glass and quartz glass substrates to fabricate a thin film chemical sensor element. Atomic Force Microscopy (AFM) and Surface Plasmon Resonance (SPR) techniques were used to characterize all the calix[4]arene LB thin films. The film thickness and the refractive index of thin films can be evaluated with the fitted experimental SPR datas. The refractive index and the thickness per monolayer of LB films were determined as a 1.58 ± 0.04 and 1.27 ± 0.09 nm, respectively. The calix[4]arene LB thin film chemical sensor element was exposed to dichloromethane, chloroform, benzene and toluene vapors. The SPR kinetic measurements displayed that, the photodetector response change, $\Delta I_{rf}$ for saturated dichloromethane vapor is much larger than the other vapors with the $\Delta I_{rf}$ value of 48 au and the diffusion coefficient value of 5.1 × $10^{-16}$ $cm^2s^{-1}$. Swelling process was analyzed by well known Fick's Equations. In this approach diffusion coefficients ($D$) for swelling were conformed to the square root of time and were correlated with the volatile organic compounds. Our results showed that calix[4]arene thin film has a highly selective with a large response to dichloromethane vapor.

**ARTICLE HISTORY**
Received March 2018
Revised April 2018
Accepted May 2018

**KEYWORDS**
calix[4]arene; swelling; surface plasmon resonance; organic vapor; LB thin film

## 1. Introduction

As the role of macrocycles in various chemistry disciplines has already been emphasized in many recent reviews over the past few years,[1–7] synthetic ones such as cyclodextrins, crown ethers, calix[n]arenes, cryptands and cucurbiturils have attracted much more growing attention from supramolecular chemistry community due to their pre-organized conformational features.[8] Since then, the efforts have been being focused on the functionalization of easily approachable macrocyclic scaffolds with established sensitive groups in search of new sensors for increasingly challenging targets. One of the favorite such macrocyclic scaffolds is calixarene representing a promising platform through versatile building blocks that has potential for applications in various fields ranging from wastewater treatment to (Quartz Crystal Microbalance) QCM modifying.[9–17] In particular, as a well-known member of calix[n]arenes family, calix[4]arene core which consists of tetraphenolic pocket forming a bowl- or cone-shaped structure with a lower (hydroxyl groups) and an upper rim (alkyl groups, *para* position to the hydroxyls) has been found to be of dramatically special interest due to its ease of synthesis and unique conformational features ensuring its high selectivity and binding efficiency toward various targets.[18–23] In general, calix[4]arene skeleton adopts one of four different conformations, that is cone, partial cone, 1,2-alternate and 1,3-alternate depending on the number and nature of modifications present both at lower and upper rims. In addition to large flexibility of these conformers provided by all these unique structural features, however, the parent calix[4]arene favorably adopts a cone/basket-like conformation due to the presence of four OH groups which provide stability to this conformation through intramolecular hydrogen-bonding interactions.[24,25] These all have been manifested by the applications of calix[4]arene architectures mainly in the area of reaction catalysis,[26,27] host-guest chemistry,[28,29] self- and co-assembling systems,[30–32] mechanically interlocked molecules,[33] nanoporous materials[34] and gas sensing applications.[35]

Among the applications mentioned above, calix[4]arene skeleton occupies a unique place in host-guest chemistry due to both acting as an assertive receptor (host) via hydrogen bonding and recognizing a substrate (guest) on the basis of structural complementarity thanks to using their molecular cavity as a reactive binding center via $\pi$-$\pi$ interactions. The success of the respective compounds in this area also allows them to participate in gas sensor applications. In this regard, these compounds may host various kinds of solvent molecules with the help of generated $\pi$-$\pi$ interactions by the aromatic fraction.[36,37] With reference to these advantages, in this study, the calix[4]arene LB films were subjected to various saturated VOCs vapors to investigate the swelling

**CONTACT** Yaser Acikbas yaser.acikbas@usak.edu.tr Faculty of Engineering, Department of Materials Science and Nanotechnology, Usak University, 64200, Usak, Turkey.

Color versions of one or more of the figures in the article can be found online at www.tandfonline.com/lmsa.

process in chemical sensor applications. Using the SPR measurement system, variations in the intensity of reflected light were monitored in real time during swelling in which organic vapor is introduced into a gas cell. Early-time Fick's law of diffusion was adopted to fit the SPR results. These results showed that calix[4]arene LB film has an excellent sensitivity and selectivity for dichloroform and may find potential applications in the development of room temperature organic vapor sensing devices.

Moving from the perspectives we mentioned extensively above, herein, we discussed our formerly developed new and highly functional calix[4]arene-based sensor offering feasibility and selectivity by combining the exceptional advantages of our analysis method and the inherent properties of calix[4]arene architecture.

## 2. Experimental

### 2.1. Materials

All starting materials, reagents and solvents used for the study were purchased either from Sigma-Aldrich/Merck or from TCI chemicals and used without further purification. The chemical sensor candidate compound, 25,27-(Dipropylmorpholinoacetamido)-26,28-dihydroxycalix[4]arene was synthesized by following the procedure reported in our previous study.[35]

### 2.2. LB film preparation

25,27-(Dipropylmorpholinoacetamido)-26,28-dihydroxycalix[4]arene (given the inset in Figure 1) was selected to fabricate a Y-type LB films using a NIMA 622 type alternate layer LB trough. Calix[4]arene was dissolved in chloroform solution to a concentration of 0.42 mg $ml^{-1}$ and 600 $\mu$l of solution spread onto the air-water interface using a Hamilton microlitre syringe. The isotherm ($\pi$-A) graph was taken with the compression speed of 30 $cm^2$ $min^{-1}$ at the room temperature.[35] This procedure repeated several times to check the reproducibility of $\pi$-A graph that used to fix the deposition pressure. Monolayer at the surface pressure of 14 mN $m^{-1}$ deposited from the air-water interface onto 50-nm thick gold-coated glass and quartz glass substrates by the alternate layer LB deposition procedure. The dipping speed for each layer was 25 mm $min^{-1}$. After the fabrication of LB films were tested using AFM and SPR measurement techniques.

### 2.3. SPR technique

The SPR measurements were performed by Surface Plasmon Resonance Spectrometer (BIOSUPLAR 6Model). Laser diode ($\lambda$ = 632.8 nm) was used as a light source in this measurements. The angular resolution of the measurement was 0.003°. A glass prism which has a reflective index n = 1.62 is mounted inside of a holder in order to be available for measurement in liquid or in air environments. The gold layer was coated homogeneously and very tiny on a glass slides. A translucent plastic flow cell was made in house for the SPR kinetic measurements. The silicon tubes were connected with the cell via two channels; inlets and outlets. The SPR system settings were controlled by a Biosuplar-Software. Measurements and data acquisition as well as data presentation were performed by the software. The photodedector response was obtained as a function of time by using single measurements, tracking mode or slope mode. Differences within both measurement channels can be shown simultaneously using this software. The SPR kinetic study was carried out by injection of dry air and organic vapor for 2 min, periodically. Thanks to WINSPALL software (developed at the Max-Plank-Institute for Polymer Research, Germany) the fitting of SPR curves was made and the specify thickness values of the calix[4]arene LB thin film could be calculated.

## 3. Results and discussion

### 3.1. Transfer ratio

LB film transfer is also a crucial parameter for monitoring deposition process and it is analyzed by calculated of the transfer ratio (*TR*).

$$TR = A_1 / A_2 \tag{1}$$

Where $A_1$ is given by reduced area of the monolayer on the water surface and $A_2$ is the area of coated film on substrate. The

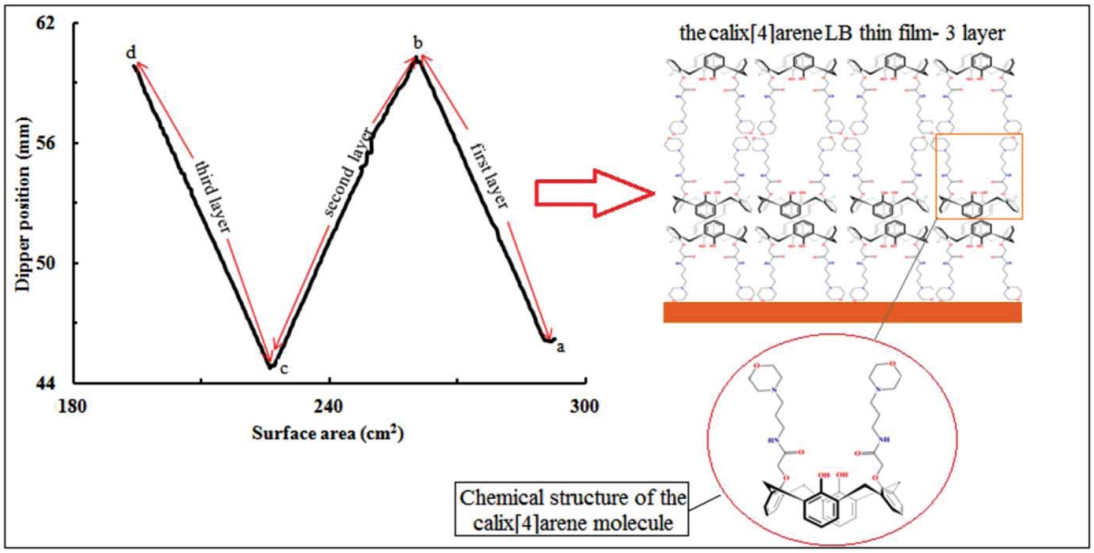


Figure 1. The deposition graphs of calix[4]arene LB film on the gold coated-glass substrate. Inset: Chemical structure of the calix[4]arene molecule.

reduced surface area change of the calix[4]arene monolayers during the deposition onto the gold-coated glass substrate for 3 bilayers is given in Figure 1. The labels of in Figure 1 are pointed from position (a) to position (b) right-to-left direction when the first LB film layer deposited onto the quartz glass substrate. Similar labelling is made for the second and third layers. Decrease of the monolayer area on the water surface for each bilayer was roughly equal to the transfer process of monolayer onto the gold-coated glass substrate. TR ratio are found to be 95% for the calix[4]arene by using Equation 1 and it suggest reproducible film deposition and good film homogeneity. It is also consistent with previous studies in the literarture where TR value was calculated over 90% for the calix[n]arene LB thin film.[38,39] As a result, monolayers based on the calix[4]arene at air-water interface are proper coating materials to use for LB film and are convenient to transfer onto different substrate such as glass, quartz crystal and a glass slide metalized on one surface with a good transfer ratio.

### 3.2. Surface plasmon resonance results

A schematic of the SPR system including an ideal curve and SPR kinetic measurement is shown in Figure 2. Thanks to this system, the film thickness and vapor sensing performance of the calix[4]arene thin films can be characterized. An index matching liquid was used for an optical contact between the calix[4]arene gold-coated glass and prism. The SPR angle (a specific angle of incidence) and curve are obtained when the plasmon waves resonate with the incident light. In this process, the incident light photons were absorbed by free electrons at the surface of the gold layer. The dependency between the experimental SPR curves and the angle of incidence ($\theta$) was monitored to see the deposition of calix[4]arene onto the gold-coated glass substrate and presented in Figure 3. It is seen that number of film layers is increased $\theta$ is also changed to larger angles and the SPR curve of the bare (uncoated) gold is taken as a reference. The linearity between the peak shifts ($\Delta\theta$) of the SPR curves and the number of layers is given as an inset graph in Figure 3. This linearity indicates that a regular deposition of calix[4]arene onto the gold-coated glass is occurred adequately and equal mass of calix[4]arene was deposited per unit area.

The film thickness and the refractive index of calix[4]arene LB films were calculated with a Fresnel formula algorithm via the Winspall software (developed by Wolfgang Knoll)[39] by fitting the experimental SPR curves. Since the calix[4]arene LB films are transparent at $\lambda = 632.8$ nm, the extinction coefficient (k) of these LB films is estimated as zero ($k = 0$).[40] The SPR curves (presented as experimentally and fitted) of the bare gold film and three-layer calix[4]arene LB films are shown in Figure 4. Same process was carried out for different number of calix[4]arene LB film layers (6 and 9 layers). All values of LB thin film thickness and the refractive index are given in Table 1. Figure 5 presents that the thickness of the calix[4]arene LB films increased linearly with the number of layers.The calix[4]arene LB film thickness and the refractive index per monolayer are found as 1.27 ± 0.09 nm and 1.58 ± 0.04 by using theoretical (the fitting data) calculations, respectively. For the refractive indices and thickness of calix[4]arene LB thin films, similar results were obtained by using the Winspall curve fitting program. The thickness of the calix[8]acid LB film is found to be 1.08 ± 0.07 nm/deposited layer with a refractive index value of 1.21 ± 0.08.[38] Values of the thickness and the refractive index of CBTEA LB films were found as 1.14 nm for the thickness per monolayer, and values between 1.64 and 1.82 for the refractive index.[39]

The inset Figure 4 shows the 3-D topographic image of the calix[4]arene molecules which coated onto the quartz glass surface. This morphological investigation of the calix[4]arene LB film (3 layers) was fixed by using the dynamic mode of AFM. The AFM results on a 4 $\mu$m x 4 $\mu$m scale show that the values of average roughness ($R_a$), a root-mean-square roughness ($R_q$) and the height of the highest peaks ($R_p$) were found as 0.73 nm, 0.45 nm and 4.92 nm, respectively. This sample exhibited nearly uniform morphology but the molecular clusters. These clusters occurred during the fabrication of the LB thin film and cause some high hills in certain areas. While this formation seems adverse situation, this morphology has proved to be very useful for vapor sensing. Thanks to this morphology, it can be promoted ingress and egress of the VOCs into and from the thin film.

### 3.3. Vapor sensing properties of the calix[4]arene LB film

Figure 6 indicates the photodetector response of the calix[4]arene LB thin film for organic vapors. The SPR kinetic study was carried out by injection of dry air and organic vapor for

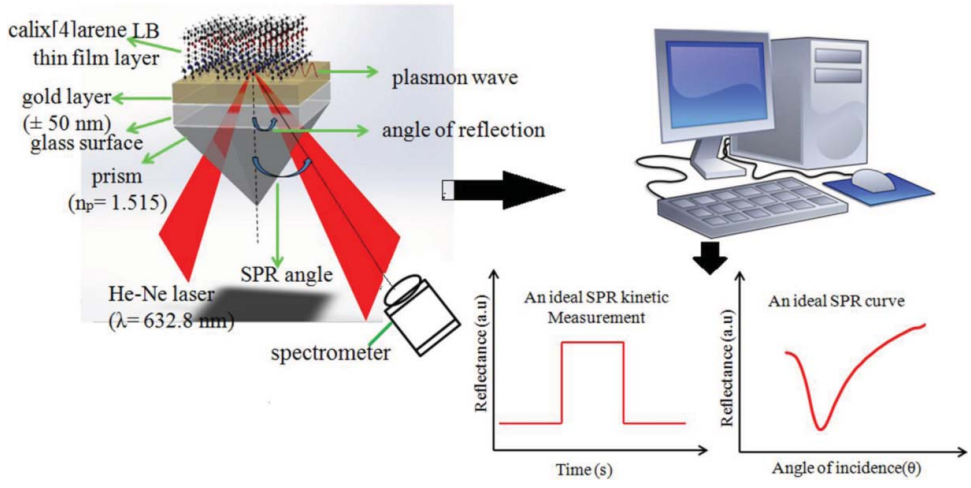


Figure 2. A schematic of the SPR system including an ideal curve and SPR kinetic measurement.

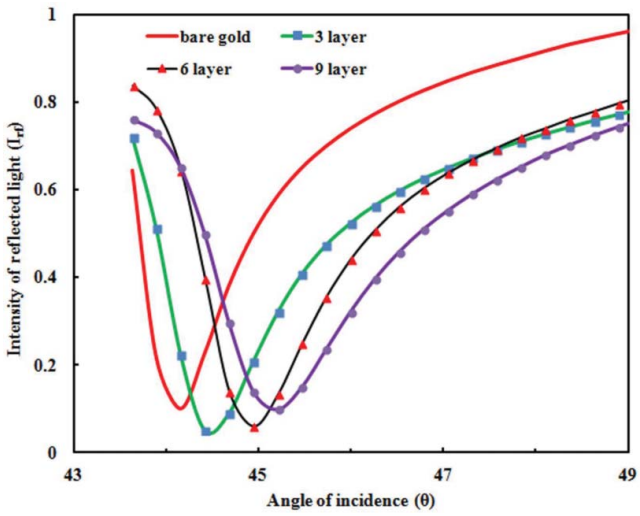


**Figure 3.** The dependency between the experimental SPR curves and the angle of incidence ($\theta$). Inset: linear increase of the peak shifts ($\Delta\theta$) as a function of number of bilayers.

2 min, periodically. Dichloromethane, chloroform, benzene and toluene were selected as harmful organic vapors for the SPR kinetic study. In the early baseline, calix[4]arene LB film sensor expose to dry air for 120 seconds and in this period of time, the response was a stable. The first response of calix[4]arene between 120 and 125s the SPR kinetic study of the calix[4]arene LB thin film increased sharply for all harmful organic vapors because of surface adsorption effect. After the vapor molecules transported into the calix[4]arene LB thin film, bulk diffusion effect plays role and the response decreased exponentially. At the time of 240s, dry air was performed, the response decreased instantaneously and then recovery process (between 240 and 244s) occurred for all harmful organic vapors due to desorption of organic vapor. The response of the calix[4] arene LB thin film sensor possesses a stable value (after 245s) and the sensor regains the first baseline. Consequently, the quick response (reproducible and reversible response) is observed to all harmful organic vapors used in SPR kinetic study. Table 2 reveals the photodetector response shift ($\Delta I_{rf}$) of the calix[4]arene LB

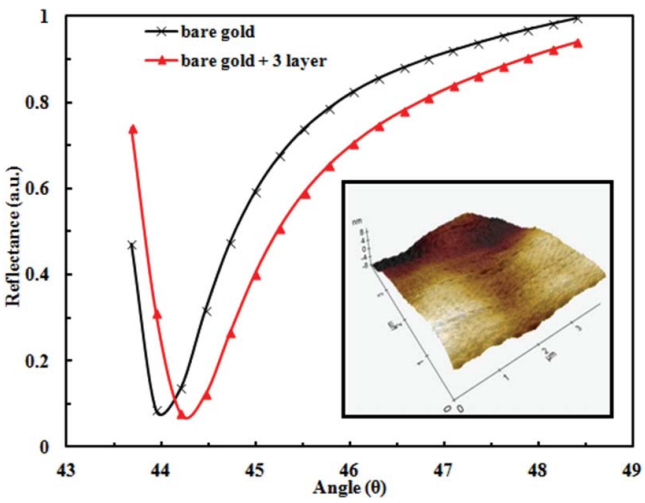


**Figure 4.** Experimentally measured (dots) and fitted (lines) SPR curves for bare gold surface and 3-layer calix[4]arene LB film. Inset: AFM image for a 3-layer LB film.

**Table 1.** The film thickness and refractive index of the calix[4]arene thin films.

| | Number of layers | Thickness (nm) | Refractive index |
|---|---|---|---|
| Calix[4]arene LB thin film | 3 | 3.60 | 1.54 |
| | 6 | 8.30 | 1.59 |
| | 9 | 11.20 | 1.63 |

thin film against harmful organic vapors and diffusion coefficients for these vapors. For each vapor, a calculation has been made and is presented in Table 2. Calix[4]arene LB thin film chemical sensor sample is observed to be significantly selective and sensitive to dichloromethane vapor compared to the chloroform, benzene and toluene vapors. All the SPR kinetic measurements of the calix[4]arene LB thin film to harmful organic vapors were carried out three times. It is fair to say that the responses of the sensor are reproducible.

The following equation[41] can be used for concentration changes in time if Fick's second law of diffusion is applied to a plane sheet and solved by assuming a constant diffusion coefficient:

$$\frac{C}{C_0} = \frac{x}{d} + \frac{2}{\pi}\sum_{n=1}^{\infty}\frac{\cos n\pi}{n}\sin\frac{n\pi x}{d}\exp\left(-\frac{Dn^2\pi^2}{d^2}t\right) \quad (2)$$

where $C_0$ and $C$are the concentration of the diffusant at time zero and $t$. $x$ corresponds to the distance at which $C$ is measured. $D$ is the diffusion coefficient and $d$ is the initial thickness of the slab. The concentration terms of the amount of diffusant can be transfered as

$$M = \int_V C dV \quad (3)$$

where $M$is the mass uptake and $V$is the volume element. If Equation 2 is considered for a plane volume element and used in Equa-

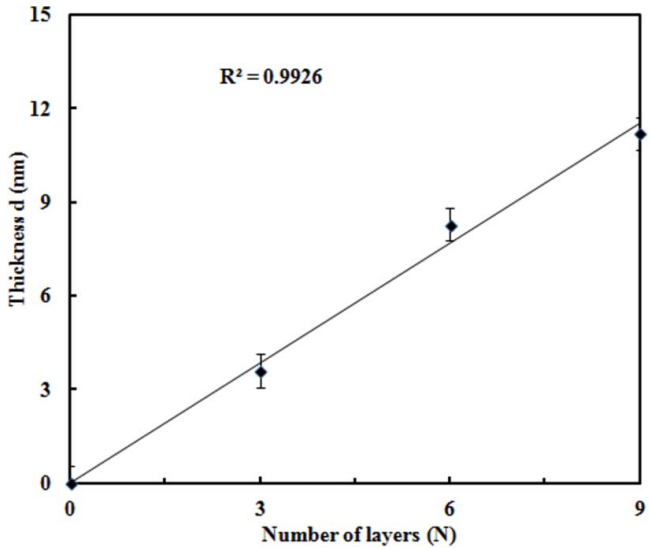


**Figure 5.** The thickness of the calix[4]arene LB layers as a function of layer.

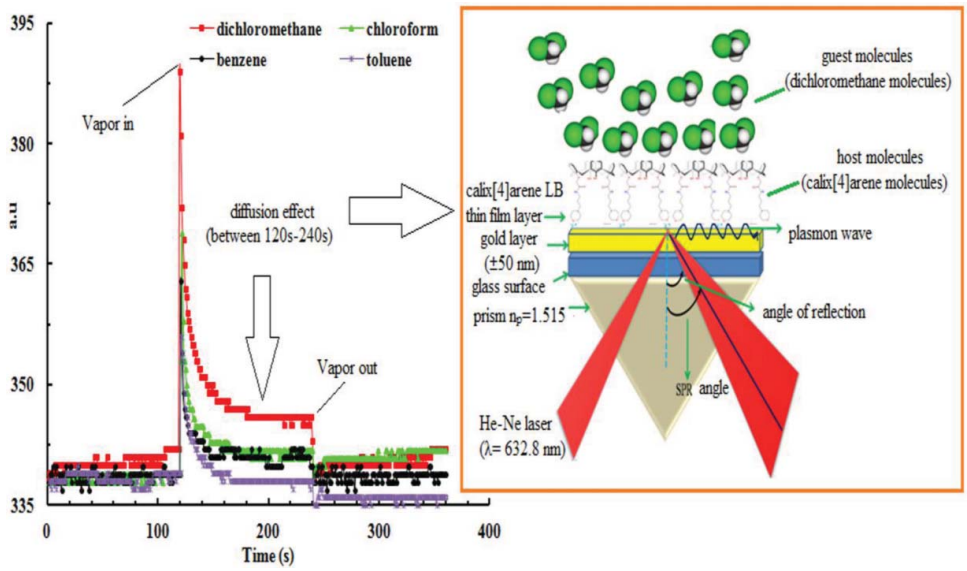


**Figure 6.** The photodetector response of the calix[4]arene LB film for organic vapors.

tion 3, the following equation can be reached.[42]

$$\frac{M_t}{M_\infty} = 1 - \frac{8}{\pi^2}\sum_{n=0}^{\infty}\frac{1}{(2n+1)^2}\exp\left(-\frac{(2n+1)^2 D\pi^2}{d^2}t\right) \quad (4)$$

where $M_t$ and $M_\infty$, represent the penetrant mass sorbed into the deposited film at time t and at equilibrium state, respectively Equation 5 represent early time approximation[43] of the Equation 4 and can be used to interpret swelling datas.

$$\frac{M_t}{M_\infty} = 4\sqrt{\frac{D}{\pi d^2}}t^{1/2} \quad (5)$$

Figure 6 shows the kinetic SPR data which is used to obtainthe calix[4]arene LB film parameters due to swelling. The normalized intensity of reflected light against swelling time where the consolidation process involves setting the time to $t = 0$ for each swelling cycle is given in Figure 7. When the duration of vapor exposure increased, the intensity of reflected light decreased. This can be explained with the chain inter diffusion between calix[4]arene chains during vapor exposure. As the saturated dichloromethane vapors penetrate into calix[4]arene LB film, the calix[4]arene chains interdiffuse and transparency of the calix[4]arene LB film increases, which results in the decrease of intensity of light reflected from the calix[4]arene LB film. These results can be concluded the amounts of diffusant entering the calix[4]arene LB film $M_t$; that is, the intensity of reflected light should be directly proportional to $M_t$.[41,44]

Equation 5 now is given by:

$$\left(\frac{M_t}{M_\infty}\right) \cong \left(\frac{I_{rf(t)}}{I_{rf(\infty)}}\right)^{-1} = 4\sqrt{\frac{D}{\pi d^2}}t^{1/2} \quad (6)$$

where $I_{rf(t)}$ and $I_{rf(\infty)}$ are the intensities of reflected light at any time, t and saturation point in $I_{rf}$, respectively. The normalized intensities of reflected light $[I_{rf(\infty)} / I_{rf(t)}]$ are plotted in Figure 8 for the square root of swelling time respect to Equation 6. The diffusion coefficients ($D_s$.) for the swelling of calix[4]arene film were found using the slopes of the linear graphs in Figure 8.

As shown in Figure 6, the photodetector response changes ($\Delta I_{rf}$) of the calix[4]arene thin film sensor for the organic vapors are observed as dichloromethane > chloroform > benzene > toluene. Also, the values of diffusion coefficient are found to be $5.10 \times 10^{-16}$ $cm^2s^{-1}$, $3.84 \times 10^{-16}$ $cm^2s^{-1}$, $2.91 \times 10^{-16}$ $cm^2s^{-1}$ and $1.99 \times 10^{-16}$ $cm^2s^{-1}$ for dichloromethane, chloroform, benzene and toluene, respectively. Similar ordering is observed both the photodetector response changes and diffusion coefficients for harmful organic vapors. The interaction between these harmful organic vapors and the calix[4]arene LB thin films is considered to be a physical absorption through a hydrogen bonding or dipole/dipole interaction.[45] The high values of the photodetector response change and diffusion coefficient are obtained for dichloromethane and chloroform vapors (chlorinated aliphatic hydrocarbons) compared with benzene and toluene vapors (aromatic hydrocarbons). This may be illuminated by the high and low dipole moment values of organic vapors and this effect is presented by previous studies in the literature.[46,47] The order

**Table 2.** The physical properties of the organic vapors.

| Organic vapors | Molar volume ($cm^3$ $mol^{-1}$) | Dipole moment (D) | Viscosity (cSt) | ($\Delta I_{rf}$) | $D(cm^2s^{-1})\times10^{-16}$ |
|---|---|---|---|---|---|
| Dichloromethane | 64.10 | 1.60 | 0.324 | 48 | 5.10 |
| Chloroform | 80.70 | 1.08 | 0.380 | 30 | 3.84 |
| Benzene | 86.36 | 0 | 0.744 | 24 | 2.91 |
| Toluene | 107.10 | 0.36 | 0.680 | 17 | 1.99 |

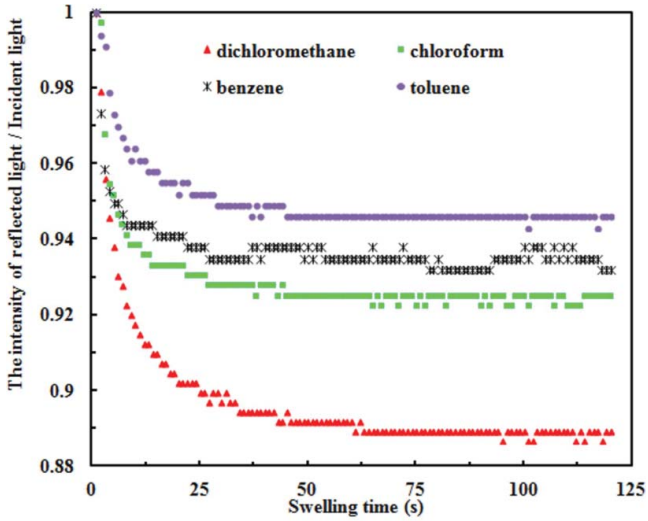


Figure 7. Normalized intensity of reflected light against swelling time, for various organic vapors.

between the values of dipole moment and the diffusion coefficient of organic vapors is similar (seen in Table 2). This can be also explained with the fact that the molar volume of toluene (107.10 $cm^3$ $mol^{-1}$) and benzene (86.36 $cm^3$ $mol^{-1}$) are bigger than the dichloromethane (64.10 $cm^3$ $mol^{-1}$) and chloroform (80.70 $cm^3$ $mol^{-1}$). While chlorinated aliphatic hydrocarbons molecules can easily diffuse into the calix[4]arene thin films, the penetration aromatic hydrocarbons molecules into the same LB films is slower and difficult (seen in Table 2 and the inset in Figure 8). Similar relationship can also be observed with the effect of viscosity. The viscosity values of aromatic hydrocarbons (0.680 and 0.744 cSt) are higher than the chlorinated aliphatic hydrocarbons (0.324 and 0.380 cSt). While benzene and toluen molecules can difficulty penetrate into calix[4]arene LB films, the diffusion of dichloromethane and chloroform molecules into the same LB films is slower. (seen in Table 2).

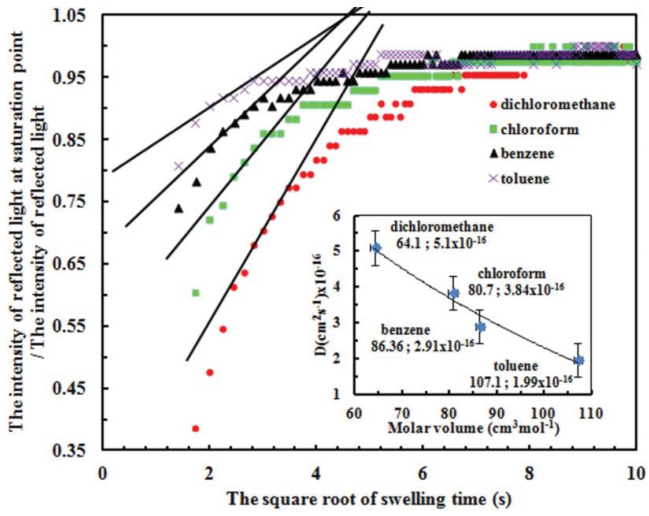


Figure 8. Plot of the intensity of reflected light against square root of swelling time, for various organic vapors.The solid line represents the fit of the data to Equation 6. Inset: A relationship between diffusion coefficient values of organic vapors and their molar volumes.

## 4. Conclusions

In this study, the calix[4]arene was characterized and investigated its chemical vapor sensing properties using AFM and SPR techniques. The calix[4]arene LB film transfer on the solid substrate has been found to be successful with a high transfer ratio of ~ 95%. Also, a linear relationship between $\Delta\theta$ and the number of the calix[4]arene LB film layer displays that the calix[4]arene molecules are deposited orderly and equal mass per unit area onto solid substrates. The refractive index and the film thickness of the calix[4]arene LB films are found to be as a 1.58 ± 0.04 and 1.27 ± 0.09 nm, respectively. SPR kinetic measurements show that the response to chlorinated aliphatic hydrocarbons (dichloromethane and chloroform vapors) is higher than the aromatic hydrocarbons (benzene and toluene) organic vapor. The SPR kinetic results can be explained with the physical parameters of organic vapors such as molar volume, viscosity and dipole moment. The response has been attributed to hydrogen bonding between the calix[4]arene LB film and the harmful organic vapor molecules or dipole/dipole interaction. The harmful chemical vapor sensing results showed that the calix[4]arene LB thin film chemical sensor element has potential applications on improving of organic vapor sensing devices.

## Funding

This work was supported by the Research Foundation of Usak University (UBAP 2017/HD-MF001). We also thank Usak University Scientific Analysis Technological Application and Research Center (UBATAM) for their support.

## References

[1] Chavez, A. D.; Evans, A. M.; Flanders, N. C.; Bispey, R. P.; Vitaku, E.; Chen, L. X.; Dichtel, W. R. Equilibration of Imine-Linked Polymers to Hexagonal Macrocycles Driven by Self-Assembly. *Chem. Eur. J.* **2018**, *24*, 1–6.

[2] Ball, M.; Zhong, Y.; Fowler, B.; Zhang, B.; Li, P.; Etkin, G.; Paley, D. W.; Decatur, J.; Dalsania, A. K.; Li, H.; Xiao, S.; Ng, F.; Steigerwald, M. L.; Nuckolls, C. Macrocyclization in the Design of Organic n-Type Electronic Materials. *J. Am. Chem. Soc.* **2016**, *138*, 12861–67.

[3] Carroll, C. N.; Naleway, J. J.; Haley, M. M.; Johnson, D. W. Arylethynyl Receptors for Neutral Molecules and Anions: Emerging Applications in Cellular Imaging. *Chem. Soc. Rev.* **2010**, *39*, 3875–88.

[4] Gross, D. E.; Zang, L.; Moore, J. S. Arylene–Ethynylene Macrocycles: Privileged Shape-Persistent Building Blocks for Organic Materials. *Pure Appl. Chem.* **2012**, *84*, 861–1112.

[5] Gong, B.; Shao, Z. Self-Assembling Organic Nanotubes with Precisely Defined, Sub-Nanometer Pores: Formation and Mass Transport Characteristics. *Acc. Chem. Res.* **2013**, *46*, 2856–66.

[6] McCaffrey, R.; Long, H.; Jin, Y.; Sanders, A.; Park, W.; Zhang, W. Template Synthesis of Gold Nanoparticles with an Organic Molecular Cage. *J. Am. Chem. Soc.* **2014**, *136*, 1782–85.

[7] Mikhailov, O. V. Molecular Structures of Metal Macrocyclic Compounds with Nitrogen, Oxygen, and Sulfur Atoms in Macrocycles Arising in Self-Assembly Processes: Quantum-Chemical Modeling. *Struct. Chem.* **2018**, *29*, 777–802. DOI: 10.1007/s11224-018-1091-7.

[8] Joseph, R.; Pulla Rao, C. Ion and Molecular Recognition by Lower Rim 1,3-Di-conjugates of Calix[4]arene as Receptors. *Chem. Rev.* **2011**, *111*, 4658–4702.

[9] Yang, F.; Wu, Y.; Ye, J.; Guo, H.; Yan, X. Novel Calixarene Benzo-15-crown-5 Derivatives: Synthesis and Complexation for Dyes. *J. Macromol. Sci., Part A: Pure Appl. Chem.* **2014**, *51*, 223–28.

[10] Ozcan, F.; Bayrakci, M.; Ertul, Ş. Synthesis and Preparation of Novel Magnetite Nanoparticles Containing Calix[4]arenes with Different

Chelating Group Towards Uranium Anions. *J. Macromol. Sci., Part A: Pure Appl. Chem.* **2015**, *52*, 599–608.
[11] Mayer, F.; Krishnan, S. T.; Schühle, D. T.; Eliseeva, S. V.; Petoud, S.; Toth, E.; Djanashvili, K. Luminescence Properties of Self-Aggregating TbIII-DOTAFunctionalized Calix[4]arenes. *Front. Chem.* **2018**, *6*, 1.
[12] Konczyk, J.; Nowik, Zajac, A.; Kozlowski, C. A. Calixarene-Based Extractants for Heavy Metal Ions Removal from Aqueous Solutions. *Sep. Sci. Technol.* **2016**, *51*, 2394–2410.
[13] Sreenivasu Mummidivarapu, V. V.; Hinge, V. K.; Pulla Rao, C. Interaction of a Dinuclear Fluorescent Cd(II) Complex of Calix[4]arene Conjugate with Phosphates and Its Applicability in Cell Imaging. *Dalton Trans.* **2015**, *44*, 1130–1141.
[14] Hrdlicka, V.; Navratil, T.; Barek, J.; Ludvik J. Electrochemical Behavior of Polycrystalline Gold Electrode Modified by Thiolated Calix[4] arene and Undecanethiol. *J. Electroanal. Chem.* **2018**, DOI: 10.1016/j.jelechem.2018.01.055.
[15] Acikbas, Y.; Dogan, G.; Erdoğan, M.; Çapan, R.; Soykan, C. Organic Vapor Sensing Properties of Copolymer Langmuir-Blodgett Thin Film Sensors. *J. Macromol. Sci., Part A: Pure Appl. Chem.* **2016**, *53*, 470–74.
[16] Acikbas, Y.; Çapan, R.; Erdoğan, M.; Cankaya, N.; Soykan, C. Characterization of N-cyclohexylmethacrylamide LB Thin Films for Room Temperature Vapor Sensor Application. *J. Macromol. Sci., Part A: Pure Appl. Chem.* **2016**, *53*, 132–39.
[17] Acikbas, Y.; Cankaya, N.; Çapan, R.; Erdoğan, M.; Soykan, C. Swelling Behavior of the 2-(4-methoxyphenylamino)-2-oxoethyl Methacrylate Monomer LB Thin Film Exposed to Various Organic Vapors by Quartz Crystal Microbalance Technique. *J. Macromol. Sci., Part A: Pure Appl. Chem.* **2016**, *53*, 18–25.
[18] Bozkurt, S.; Durmaz, M.; Sırıt, A.; Yılmaz, M. Synthesis of Calix[4] arene Mono and Diamide Derivatives and Selective Complexation of Alkali and Alkaline Earth Cations. *J. Macromol. Sci., Part A: Pure Appl. Chem.* **2007**, *44*, 159–65.
[19] Karakücük, A.; Kocabas, E.; Sırıt, A.; Memon, S.; Yılmazi M.; Roundhill, D. M. Polymer Supported Calix[4]arene Schiff Bases: A Novel Chelating Resin for $Hg^{2+}$ and Dichromate Anions. *J. Macromol. Sci., Part A: Pure Appl. Chem.* **2005**, *42*, 691–704.
[20] Fong, A.; McCormick, L.; Teat, S. J.; Brechin, E. K.; Dalgarno, S. J. Exploratory Studies into 3d/4f Cluster Formation with Fully Bridge-Substituted Calix[4]arenes. *Supramol. Chem.* **2018**, *30*, 504–9. DOI: 10.1080/10610278.2018.1430894.
[21] Du, Y.; Li, X.; Zheng, H.; Lv, X.; Jia, Q. *Anal. Chim. Acta.* **2018**, *1001*, 134–42.
[22] Nehra, A.; Yarramala, D. S.; Bandaru, S.; Pulla Rao, C. Cyclohexyl-Diimine Capped Lower Rim 1,3-di-Derivatized Calix[4]arene Conjugate as Sensor for $Al^{3+}$ by Spectroscopy, Microscopy, Titration Calorimetry and DFT Computations. *Supramol. Chem.* **2018**, *30*, 619–26. DOI: 10.1080/10610278.2018.1424851.
[23] Jang, Y.-M.; Yu, C.-J.; Kim, J.-S.; Kim, S.-U. Ab Initio Design of Drug Carriers for Zoledronate Guest Molecule Using Phosphonated and Sulfonated Calix[4]arene and Calix[4]resorcinarene Host Molecules. *J. Mater. Sci.* **2018**, *53*, 5125–5139.
[24] Naseer, M. M.; Ahmed, M.; Hameed, S. Functionalized Calix[4]arenes as Potential Therapeutic Agents. *Chem. Biol. Drug Des.* **2017**, *89*, 243–56.
[25] Matthews, S. E.; Cecioni, S.; O¢Brien, J. E.; MacDonald, C. J.; Hughes, D. L.; Jones, G. A.; Ashworth, S. H.; Vidal, S. Fixing the Conformation of Calix[4]arenes: When Are Three Carbons Not Enough? *Chem. Eur. J.* **2018**, *24*, 1–10.
[26] Akceylan, E.; Yılmaz, M. *J. Macromol. Sci., Part A: Pure Appl. Chem.* **2012**, *49*, 911–17.
[27] da Silva Abranches, P. A.; de Paiva, W. F.; de Fatima, A.; Martins, F. T.; Fernandes, S. A. Calix[n]arene-Catalyzed Three-Component Povarov Reaction: Microwave-Assisted Synthesis of Julolidines and Mechanistic Insights. *J. Org. Chem.* **2018**, *83*, 1761–71.
[28] Bai, X.; Yang, F.; Xie, J.; Guo, H. Novel 1,2-3,4-Bridged and 1,3-Bridged Calix[4]arene Based on Large s-triazine Conjugate Systems: Synthesis and Complexation for Dyes. *J. Macromol. Sci., Part A: Pure Appl. Chem.* **2013**, *50*, 334–39.
[29] Pang, H.; Xu, P.; Li, C.; Zhan, Y.; Zhang, Z.; Zhang, W.; Yang, G.; Sun, Y.; Li, H. A Photo-Responsive Macroscopic Switch Constructed Using a Chiral Azo-Calix[4]arene Functionalized Silicon Surface. *Chem. Commun.* **2018**, *54*, 2978–81. DOI: 10.1039/c8cc01196f.
[30] Yu, X.; Tu, C.; He, L.; Wang, R.; Sun, G.; Yan, D.; Zhu, X. Self-assembly of Supramolecular Amphiphile Constructed by Hydrophilic Calix[4]arene Derivative and Phenol Palmitate. *J. Macromol. Sci., Part A: Pure Appl. Chem.* **2009**, *46*, 360–67.
[31] Rodler, F.; Schade, B.; Jager, C. M.; Backes, S.; Hampel, F.; Böttcher, C.; Clark, T.; Hirsch, A. Amphiphilic Perylene–Calix[4]arene Hybrids: Synthesis and Tunable Self-Assembly. *J. Am. Chem. Soc.* **2015**, *137*, 3308–17.
[32] Choi, H.; Seo, H.; Go, M.; Lee, S. S.; Jung, J. H. Enhanced Mechanical and Helical Properties with Achiral Calix[4]arene in Co-Assembled Hydrogel which Exhibited the Helical Structure. *Eur. J. Org. Chem.* **2018**, *2018*, 219–22.
[33] Zhang, M.; Yan, X.; Huang, F.; Niu, Z.; Gibson, H. W. Stimuli-Responsive Host–Guest Systems Based on the Recognition of Cryptands by Organic Guests. *Acc. Chem. Res.* **2014**, *47*, 1995–2005.
[34] Brancatelli, G.; De Zorzi, R.; Hickey, N.; Siega, P.; Zingone, G.; Geremia, S. New Multicomponent Porous Architecture of Self-Assembled Porphyrins/Calixarenes Driven by Nickel Ions. *Cryst. Growth Des.* **2012**, *12*, 5111–17.
[35] Acikbas, Y.; Bozkurt, S.; Halay, E.; Capan, R.; Guloglu, M. L.; Sirit, A.; Erdogan, M. Fabrication and Characterization of Calix[4]arene Langmuir–Blodgett Thin Film for Gas Sensing Applications. *J. Incl. Phenom. Macrocycl. Chem.* **2017**, *89*, 77–84.
[36] Moris, S.; Galdamez, A.; Jara, P.; Saitz-Barria, C. Synthesis of Novel p-tert-Butylcalix[4]arene Derivative: Structural Characterization of a Methanol Inclusion Compound. *Crystals* **2016**, *6*, 114–123.
[37] Surov, O. V.; Krestianinov, M. A.; Voronova, M. I. Complexation of Solvents and Conformational Equilibria in Solutions of the Simplest Calix[4]arenes. *Spectrochim. Acta, Part A.* **2015**, *134*, 121–26.
[38] Çapan, R.; Özbek, Z.; Göktaş, H.; Şen, S.; İnce, F. G.; Özel, M. E.; Stanciu, G. A.; Davis, F. Characterization of Langmuir-Blodgett Films of a Calix[8]arene and Sensing Properties Towards Volatile Organic Vapors. *Sens. Actuators B* **2010**, *148*, 358–365.
[39] Özbek, Z.; Çapan, R.; Göktaş, H.; Şen, S.; İnce, F. G.; Özel, M. E.; Davis, F. Optical Parameters of Calix[4]arene Films and Their Response to Volatile Organic Vapors. *Sens. Actuators B* **2011**, *158*, 235–240.
[40] Hassan, A .K.; Nabok, A. V.; Ray, A. K.; Lucke, A.; Smith, K.; Stirling, C. J. M.; Davis, F. Thin Films of Calix-4-resorcinarene Deposited by Spin Coating and Langmuir-Blodgett Techniques: Determination of Film Parameters by Surface Plasmon Resonance. *Mater. Sci. Eng. C* **1999**, *8–9*, 251–255.
[41] Erdogan, M.; Capan, R.; Davis, F. F. Swelling Behaviour of Calixarene Film Exposed to Various Organic Vapours by Surface Plasmon Resonance Technique. *Sens. Actuators B.* **2010**, *145*, 66–70.
[42] Crank, J. *The Mathematics of Diffusion*; Oxford University Press: London, **1970**.
[43] Acikbas, Y.; Taktak, F.; Tuncer, C.; Bütün, V.; Capan, R; Erdogan, M. Characterization of PDPA-b-PDMA-b-PDPA Triblock Copolymer Langmuir-Blodgett Films for Organic Vapor Sensing Application. *Mol. Cryst. Liq. Cryst.* **2016**, *634*(1), 104–117.
[44] Acikbas, Y.; Erdogan; Capan, R; Yukruk, F. Optical Characterization of N,N'-dicyclohexyl-3,4:9,10-perylene bis(Dicarboximide) Langmuir-Blodgett Film for Determination of Volatile Organic Compounds. *Anal. Lett.* **2016**, *49*(16), 2573–2586.
[45] Çapan, İ.; İlhan, B. Gas Sensing Properties of Mixed Stearic Acid/Phthalocyanine LB Thin Films Investigated Using QCM and SPR. *J. Optoelectron. Adv. Mater.* **2015**, *17*, 456–461.
[46] Ichinohe, S.; Tanaka, H.; Kanno, Y. Gas Sensing by AT-cut Quartz Crystal Oscillator Coated with Mixed-Lipid Film. *Sens. Actuators B* **2007**, *123*, 306–312.
[47] Ceyhan, T.; Altındal, A.; Özkaya, A. R.; Erbil, M. K.; Bekaroğlu, Ö. Synthesis, Characterization, and Electrochemical, Electrical and Gas Sensing Properties of a Novel Tert-butylcalix[4]arene Bridged Bis Double-Decker Lutetium(III) Phthalocyanine. *Polyhedron* **2007**, *26*, 73–84.